d-wave anisotropy and coexistence of the superconducting gap and pseudogap in $La_{2-x}Sr_xCuO_4$/Ag junctions

T. Miyake, T. Imaizumi, and I. Iguchi
Department of Physics, Tokyo Institute of Technology, 2-12-1 O-okayama, Meguro-ku, Tokyo 152-8551, Japan
(Received 29 July 2003; revised manuscript received 6 October 2003; published 30 December 2003)

We present the angle-resolved tunneling spectroscopy of $La_{2-x}Sr_xCuO_4$ (LSCO)/Ag junctions. The observed tunnel conductance curves show the superconducting gap (SG) at 9 ± 1 mV for the near optimally doped samples and at 11 ± 1 mV for the underdoped samples. They also show strong decrease of conductance at a few tens of mV corresponding to the possible pseudogap (PG) for zero- and finite-angle junctions. Besides, the zero bias conductance peak (ZBCP) is observable for finite-angle junctions. The simultaneous observation of SG, PG, and ZBCP implies the coexistence of superconducting gap and pseudogap with the *d*-wave order parameter for LSCO.

DOI: 10.1103/PhysRevB.68.214520 PACS number(s): 74.50.+r, 74.25.Jb, 74.72.Dn, 74.78.Bz

I. INTRODUCTION

There have been a lot of studies on high-T_c oxide superconductors. It is, however, instructive to point out that most of the surface measurements such as the scanning tunneling spectroscopy (STM), phase sensitive measurement, tunnel junction spectroscopy or angle-resolved photoemission spectroscopy (ARPES) have been mainly limited to Bi oxides since the Bi-oxide crystals are easily cleaved and provide the fresh surface. $La_{2-x}Sr_xCuO_4$ (LSCO) is considered to be a basic material among high-T_c superconductors. For LSCO oxides, however, single crystals cannot be easily cleaved and the growth of thin films of high quality is also hard. Due to these difficulties, there has been no direct experimental evidence clarifying its pairing symmetry such as performed by the phase sensitive measurements,[1–4] although evidence for the *d*-wave symmetry has been given by the measurements using nuclear magnetic resonance,[5–7] ARPES,[8] neutron scattering,[9] etc. Some symmetry discussion based on the measured zero bias conductance peak (ZBCP) at the (110) crystal direction only is given,[10] but it is not conclusive. We point out that the ZBCP also appears as the junction circuit of a normal diffusive metal as well as the Andreev bound states.[11]

As for the tunnel-gap measurement, there exist some scattered data at an early stage of high-T_c discovery using STM or a tunnel junction.[12–14] Recently, some measurement was reported using an improved STM technique,[15] but still far from a systematic study. We note that the STM technique detects a very small limited area, whose result strongly depends on the microscopic surface condition in films and crystals, so the correct information including spatial inhomogeneities would be only obtained by scanning some finite area.

If LSCO has a $d_{x2\text{-}y2}$-wave pairing symmetry, the fourfold order parameter symmetry will be reflected in the junction property in the same way as the case of $YBa_2Cu_3O_{7-y}$ (YBCO) material, i.e., the tunnel conductance depends on the angle between the junction interface and the crystal orientation of the high-T_c electrode. Using the ramp-edge junction technique, we have recently developed a fabrication technique of high quality YBCO/Ag junctions capable of angle-resolved tunnel spectroscopy, which demonstrated the $d_{x2\text{-}y2}$-wave nature of YBCO superconductors.[16,17] The ramp-edge junction,[18,19] different from a conventional sandwich-type tunnel junction, relies on the formation of new fresh junction surface by an Ar ion milling process and *in situ* deposition of the counterelectrode, which yields junctions of high quality.[20] The angle-dependent tunnel gap structures and the formation of Andreev bound states are also expected for LSCO.

In this paper, we present the tunnel conductance characteristics observed in the reproducible LSCO/Ag junctions fabricated using a ramp-edge technique. Clear gap structures which represent the coexistence of the superconducting gap (SG) and the pseudogap (PG) were observable. The results suggest that the superconducting state consists of SG and PG regions. Moreover, the tunnel-gap structure depended on the junction angle geometry and the ZBCP due to the formation of Andreev bound states was observable. The simultaneous observation of SG, PG, and ZBCP for the same measurements provides strong evidence that the LSCO superconductor has a predominant $d_{x2\text{-}y2}$-wave pairing symmetry and suggests the possible inhomogeneous state in space.

II. EXPERIMENT

The samples were fabricated in the following way. First, a LSCO film about 100 nm thick and an insulating $LaSrAlO_4$ layer about 100 nm thick were deposited subsequently on an $LaSrAlO_4(001)$ single crystal substrate at 640 °C under an oxygen pressure of 50 mTorr by a pulsed laser deposition technique using a KrF excimer laser with a wavelength of 248 nm. The pulse repetition frequency was 1 Hz and the laser energy was 280 mJ. We used two different targets with $x=0.15$ corresponding to an optimal doping regime and $x=0.09$ corresponding to an underdoping regime. The $LaSrAlO_4$ substrate ($a=0.3755$ nm) was used because of the best crystal matching to LSCO ($a=0.3777$ nm). The x-ray diffraction pattern showed a strong *c*-axis orientation. For near optimally doped samples, the *c*-axis length was 1.325 nm. Then, using photolithography and an Ar ion milling technique, the ramp-edge structure was formed. The beam voltage and current were 250 V and 4.0 mA, respectively.

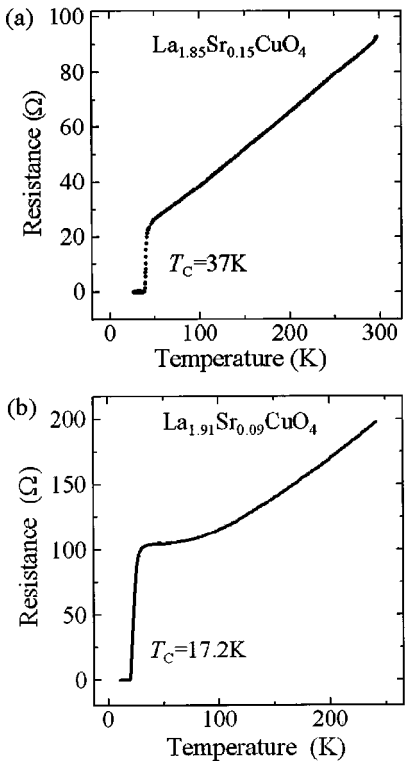

FIG. 1. Resistance vs temperature curves for LSCO thin-film electrodes deposited using (a) an optimally doped target ($x=0.15$) and (b) an underdoped target ($x=0.09$) after the junction fabrication.

The beam angle against the sample surface was 35°. After removing the photoresist, the surface was cleaned by Ar ion bombarding (~150 V) with a beam angle of 10° for a few minutes, and an Ag film 100–200 nm thick was deposited *in situ* subsequently. Then the films were patterned into the ramp-edge junction structure with a width w of 10–50 μm. Finally, the post annealing was done at 350 °C under oxygen pressure of 50 mTorr. The effective junction area was 2–4 μm^2. The junction barrier was considered to be natively formed between LSCO and Ag films. The measurements were performed using a conventional four-probe method. The derivative characteristics were obtained using a digital lock-in amplifier.

III. RESULTS AND DISCUSSION

Figure 1 shows examples of resistance vs temperature (*R-T*) curves for the LSCO thin film electrodes using the optimally doped target ($x=0.15$) and an underdoped target ($x=0.09$) after the junction fabrication. For thin films grown using the optimally doped target, T_c of 37 K was attained and the *R-T* curve exhibited a typical linear metallic behavior. The T_c value using the optimally doped target ranged from 31 to 37 K. On the other hand, for those grown using the underdoped target, lower T_c (17–27 K) was obtained. The *R-T* curve exhibited downward bending behavior typical to an underdoped superconductor.

Figure 2 shows the tunnel conductance curves observed for two LSCO/Ag junction samples with different angle geometries at 4.2 K: one with $\alpha=0°$ ($w=10\ \mu$m, $T_c=23$ K) (a) and the other with $\alpha=15°$ ($w=50\ \mu$m, $T_c=34$ K) (b), where α is the angle between the LSCO *a* axis and the junction interface as shown in Fig. 2. The junction resistances of (a) and (b) were 100 and 40 Ω, respectively. A clear gap structure was observable for the $\alpha=0°$ junction and the ZBCP typical of the *d*-wave symmetry was recognized for the 15° junction. The sharp appearance of a ZBCP suggests that the fabricated LSCO junctions were of high quality with the least disorder.

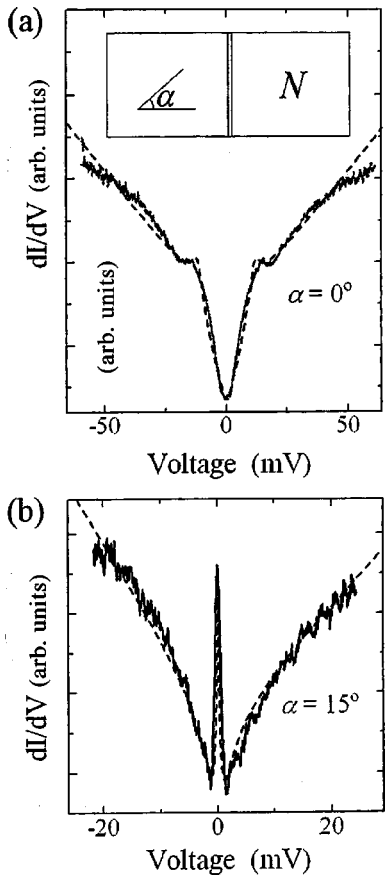

FIG. 2. Tunnel conductance curves for two LSCO/Ag junctions with $\alpha=0°$ and $\alpha=15°$ at 4.2 K. The fitting curves were calculated using the BTK theory extended to the anisotropic *d*-wave superconductor with taking the gap broadening parameter γ due to the quasiparticle scattering effect into account.

To compare the observed experimental data with a theoretical model, we have calculated the tunnel conductance between a superconductor and a normal metal based on the anisotropic *d*-wave model. The general expression is given by the extended Blonder-Tinkham-Klapwijk theory.[21] In a high-barrier approximation, the differential tunnel conductance related to the electronic density of states, taking the gap broadening parameter γ due to the quasiparticle scattering effect[22] into account, is given by

$$\sigma_T(E)=\frac{\int_{-\pi/2}^{\pi/2} d\theta \sigma_N(\theta)\sigma_R(E,\theta)\cos\theta}{\int_{-\pi/2}^{\pi/2} d\theta \sigma_N(\theta)\cos\theta}, \qquad (1)$$

$$\sigma_R(E,\theta)=\frac{1+\sigma_N(\theta)|\Gamma_+|^2+(\sigma_N(\theta)-1)|\Gamma_+\Gamma_-|^2}{|1+(\sigma_N(\theta)-1)\Gamma_+\Gamma_-\exp(i\varphi_- - i\varphi_+)|^2}, \tag{2}$$

where $\sigma_N(\theta)=\cos^2\theta/(\cos^2\theta+Z^2)$, $\Gamma_\pm=[E-i\gamma-\sqrt{(E-i\gamma)^2-\Delta^2(\theta_\pm)}]/|\Delta(\theta_\pm)|$, $e^{i\varphi_\pm}=\Delta(\theta_\pm)/|\Delta(\theta_\pm)|$, Z is the barrier parameter, and $\Delta(\theta_\pm)$ is an anisotropic order parameter.

In the above equations, it is emphasized that the junction conductance depends on Z and generally does not coincide with the bulk tunnel conductance. The data fitting was done by considering the contribution of the linear background conductance typical as high-T_c superconductors in Eqs. (1) and (2). The best fits were obtained with $\Delta_{SG}=11.5$ meV and $\gamma=1.2$ meV for the $\alpha=0°$ junction and $\Delta_{SG}=10$ meV and $\gamma=3.3$ meV for the $\alpha=15°$ junction. The agreements are reasonably good. We also point out that the gap value as obtained by fitting Eqs. (1) and (2) gives a value very close to the one at the gap hump in the conductance curve when γ is not large. The clear appearance of a gap structure in Fig. 2(a) and its smeared appearance in Fig. 2(b) are due to the difference in magnitude of the gap broadening parameter γ. The magnitude of γ may depend on either the junction quality or the interface condition.

The calculation based on Eqs. (1) and (2) showed that the ZBCP appears clearly for any finite angle of α, even at $\alpha=3°$. The observed gap for the junction utilizing the near optimally doped LSCO films was slightly smaller than that of the underdoped ones. The similar tendency has been reported for Bi2212 crystals using ARPES.[23] The gap value of 11 meV yields a large value of $2\Delta/k_BT_c\approx 11$ for the underdoped samples, which might be comparable to the previously reported values.[10]

The amount of carrier doping in the LSCO thin films depended on the film deposition condition and the junction fabrication process involving photolithography and Ar ion milling techniques. The effective doping level after the junction formation was estimated from the value of T_c, the *c*-axis length and the behavior of the resistivity vs temperature (*R*-*T*) curve of the thin film electrode. For example, for the underdoped films, T_c is relatively low and the *c*-axis length becomes relatively shorter and the *R*-*T* curve exhibits downward bending behavior as shown in Fig. 1(b). The effective doping levels for the samples of Figs. 1(a) and 1(b), by comparing them with the reported data,[24] are judged to be $x\sim 0.1$ for the underdoped one and $x\sim 0.14$ for the near optimally doped one, respectively.

For the possible contribution of the strain field induced effect of LSCO thin films[24] to an anisotropic effect, it is not likely since we always observed the ZBCP for the junctions with any finite angle α different from 0°, but not with $\alpha=0°$. In case of the involvement of strain effect in the pairing anisotropy, the ZBCP should also appear for the junctions with $\alpha=0°$.

Figure 3 shows a comparison of the tunnel conductance curves observed for junctions with two different angle geometries ($\alpha=0°$ and $\alpha=45°$) fabricated on the same substrate simultaneously. The junction resistance was about 100 Ω for both junctions. The ZBCP was only observable for the $\alpha=45°$ junction, again indicating that LSCO is a $d_{x2\text{-}y2}$-wave superconductor. The result is quite similar to those observed for YBCO junctions,[16] reflecting that LSCO and YBCO superconductors belong to the same class of cuprate among the high-T_c superconductors. The SG structures indicated by the arrows appeared much more distinctly for the $\alpha=0°$ junction than for the $\alpha=45°$ junction.

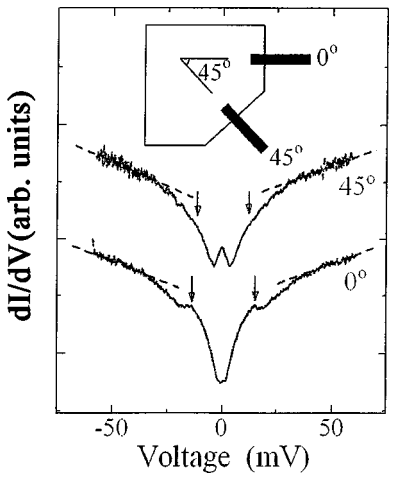

FIG. 3. Tunnel conductance curves for LSCO/Ag junctions with $\alpha=0°$ at 4.2 K and $\alpha=45°$ at 9.8 K fabricated on the same substrate simultaneously. The arrows indicate the superconducting gap structures. The strong decrease from the background linear conductance (dashed lines) was recognized at voltages about a few tens of mV.

The appearance of a gap structure or a small depression in the tunnel conductance at the gap voltage even for the 45° junction is theoretically predicted.[25–27] The structure at the gap voltage depends on the barrier height and temperature. When the barrier height is large, it gives a strong peak, whereas when the barrier height is small, this structure is smeared and gives a remaining depression in the curve.[28] For example, in Ref. 27, a clear peak at the gap is recognized even at the 45° angle geometry. The peak at the gap voltage appears because the tunneling occurs from various directions even for the 45° geometry. In the case when the quasiparticles are incident only in the 45° direction, the peak or the depression may not be observed, but the actual junction geometry precludes such a possibility.

In addition to the SG structures indicated by the arrows, a strong decrease from the background conductance (dashed lines), suggesting the opening of another gap, was also recognized at voltages of a few tens of mV. They appeared at voltages much greater than the superconducting gap; hence may be attributed to the possible PG of LSCO. We have determined the PG value from a visual inspection, as many authors did before, since a detailed density of states for the PG is not known. Note that such conductance decrease around 35 mV is also recognized in Fig. 1(a). The PG in the tunneling spectroscopy usually appears as a conductance decrease without accompanying the bump structure.[29] The same order of magnitude of PG has also been observed in the ARPES. This sample was the underdoped one with $x\sim 0.1$,

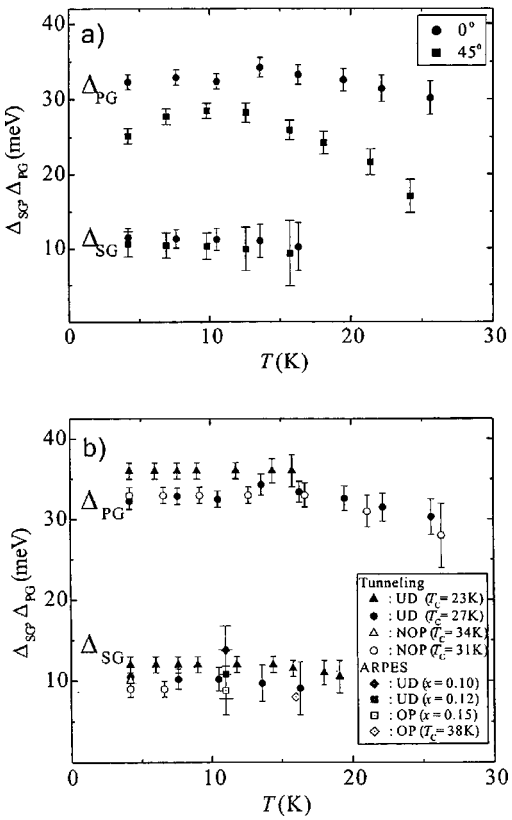

FIG. 4. (a) Temperature dependence of the superconducting gap parameter (Δ_{SG}) and the pseudogap parameter (Δ_{PG}) for LSCO/Ag junctions with $\alpha=0°$ and 45° angle geometries. (b) Summary plot of Δ_{SG} and Δ_{PG} as a function of temperature for several junctions $\alpha=0°$, together with the data by ARPES for comparison. Note that OP, NOP, and UD mean optimally doped, near optimally doped, and underdoped, respectively. The data points □, ■, and ◆ were obtained from Ref. 23, and ◇ was obtained from Ref. 30.

as judged from $T_c=23$ K. $c=1.3207$ nm and a downward bending behavior of the *R-T* curve.

In contrast to the fact that the SG and PG for Bi2212 material appeared at about the same voltage,[29,31,32] those for LSCO appeared quite different. There seems to be no correlation between the SG and PG. The observed tunnel conductance is given by the sum of contribution from the SG region and that from the PG region, i.e., a parallel tunneling regime. The results suggest that the coexistence of SG and PG in the LSCO thin film, being consistent with the recent observation of microscopic SG and PG domains in space in Bi2212 single crystals by STM measurements.[33,34]

Figure 4(a) shows the magnitude of the superconducting gap parameter (Δ_{SG}) and the pseudogap parameter (Δ_{PG}) as a function of temperature for the sample in Fig. 3. The Δ_{SG} value for the $\alpha=0°$ junction was obtained by fitting the calculated curve with the gap broadening factor γ. The observed Δ_{SG} value changed slightly with increasing temperature, but became smeared at temperatures close to T_c. On the other hand, the Δ_{PG} value was roughly constant for the $\alpha=0°$ junction, while it appreciably decreased toward T_c for the $\alpha=45°$ junction. The Δ_{PG} for the $\alpha=0°$ junction never seems to approach Δ_{SG} even near T_c. The result reflects that

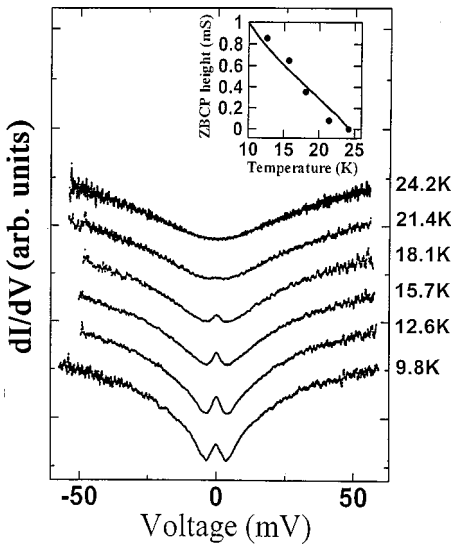

FIG. 5. Tunnel conductance curves for LSCO/Ag junctions with $\alpha=45°$ in Fig. 3 at different temperatures. The inset shows the zero bias conductance peak ZBCP height, together with the calculated curve based on the *d*-wave theory as a function of temperature.

the origins of SG and PG seem to be different. It is also even hard to say whether the SG gap vanishes at T_c or not, because of increase of the uncertainty in the gap value.

Figure 4(b) summarizes the observed results for the near optimally doped and underdoped samples with $\alpha=0°$ together with those of ARPES results for comparison. The observed SG data seem to be consistent with the ARPES data. The difference in Δ_{SG} between the underdoped and near optimally doped samples was about 20% [$\Delta_{SG}=9\pm1$ meV for near optimally doped (NOP) samples, $\Delta_{SG}=11\pm1$ meV for underdoped (UD) samples], which might be comparable to 30–40 % for the ARPES data. Note that the $\alpha=0°$ junctions were free from the ZBCP. The SG was considerably smeared at higher temperature closer to T_c, which precluded the estimate of Δ since γ became large ($\gamma\sim\Delta$).

The PG structure was observable at least up to T_c. The measurement above T_c, however, could not be performed since the large contribution of the normal electrode resistance of the LSCO film in the ramp-edge junction geometry came in above T_c, which made the separate measurement of junction resistance almost impossible. The PG in the ARPES (Ref. 30) was measured above T_c. Hence it is not appropriate to compare these two PG gaps directly. They may be qualitatively different, since the latter connects to the SG below T_c smoothly.

Figure 5 shows the temperature dependence of tunnel conductance for the 45° junction in Fig. 3. It is understood that the ZBCP decreased with increasing temperature. In the inset of Fig. 5, the ZBCP height was plotted as a function of temperature. In the model calculation, the following zero-bias conductance formula obtained by extending the *d*-wave theory to finite temperature case was used,

$$\left.\frac{dI}{dV}\right|_{V=0} \propto -\int_{-\pi/2}^{\pi/2} d\theta g(\theta) \int_{-\infty}^{\infty} dE \left.\frac{\partial f(E-eV)}{\partial V}\right|_{V=0} \times \sigma_R(E,\theta,T), \quad (3)$$

where $f(E)=1/(e^{E/k_BT}+1)$ and $g(\theta)=\cos\theta$ is the weighting factor for the incident angle of quasiparticles at the interface. The data fitting was done using the observed parameters and the barrier parameter of $Z=2$. The agreement between the experiment and theory is reasonably good, demonstrating the predominant $d_{x2\text{-}y2}$-wave symmetry for LSCO material.

IV. CONCLUSIONS

In summary, we have reported the tunneling spectroscopy of angle-resolved $La_{2-x}Sr_xCuO_4$/Ag junctions. The tunnel conductance curves showed bump peaks corresponding to the superconducting gap, strong local decrease of conductance corresponding to the pseudogap structure and the ZBCP. The observed results are consistent with the recent STM and ARPES results. The simultaneous observation of SG, PG, and ZBCP implies the coexistence of superconducting gap and pseudogap with the *d*-wave order parameter for LSCO.

ACKNOWLEDGMENTS

The authors are very grateful to Professor Y. Tanaka for helpful discussions. This work was supported by a Grant-in-Aid for Scientific Research of the Ministry of Education, Culture, Sports, Science and Technology.

[1] D. A. Wollman, D. J. Van Harlingen, W. C. Lee, D. M. Ginsberg, and A. J. Leggett, Phys. Rev. Lett. **71**, 2134 (1993).
[2] C. C. Tsuei and J. R. Kirtley, Rev. Mod. Phys. **72**, 969 (2000).
[3] I. Iguchi and Z. Wen, Phys. Rev. B **49**, 12 388 (1994).
[4] A. Sugimoto, T. Yamaguchi, and I. Iguchi, Physica C **367**, 28 (2002).
[5] H. Yasuoka, S. Kambe, Y. Itoh, and T. Machi, Physica B **199**, 278 (1994).
[6] N. Pyka, W. Reichardt, L. Pintschoviuo, G. Engle, J. Rossat-Mignod, and J. Y. Henry, Phys. Rev. Lett. **70**, 1457 (1993).
[7] Z-X. Shen, D. S. Dessau, B. O. Welles, D. M. King, W. E. Spicer, A. J. Arko, D. Marshall, L. W. Lombarda, A. Kapitulnik, P. Dickinson, S. Doniach, J. Dicaarlo, A. G. Loeser, and C. H. Park, Phys. Rev. Lett. **70**, 1553 (1993).
[8] K. Yamada, S. Wakimoto, C. H. Lee, M. A. Kastner, S. Hosoya, M. Greven, Y. Endoh, and R. J. Birgeneau, Phys. Rev. Lett. **75**, 1626 (1995).
[9] A. Ino, C. Kim, M. Nakamura, T. Yoshida, T. Mizokawa, A. Fujimori, Z.-X. Shen, T. Kakeshita, H. Eisaki, and S. Uchida, Phys. Rev. B **65**, 094504 (2002).
[10] N.-C. Yeh, J. Y. T. Wei, C.-T. Chen, W. D. Si, and X. X. Xi, Physica C **341–348**, 1639 (2000).
[11] Y. Tanaka, Yu. V. Nazarov, and S. Kashiwaya, Phys. Rev. Lett. **90**, 167003 (2003).
[12] J. R. Kirtley, C. C. Tsuei, Sung I. Park, C. C. Chi, J. Rozen, and M. W. Shafer, Phys. Rev. B **35**, 7216 (1987).
[13] A. P. Fein, J. R. Kirtley, and M. W. Shafer, Phys. Rev. B **37**, 9738 (1988).
[14] M. Naito, D. P. E. Smith, M. D. Kirk, B. Oh, M. R. Hahn, K. Char, D. B. Mitzi, J. Z. Sun, D. J. Webb, M. R. Beasley, O. Fischer, T. H. Geballe, R. H. Hammond, A. Kapitulnik, and C. F. Quate, Phys. Rev. B **35**, 7228 (1987).
[15] M. Oda, T. Matsuzaki, N. Momono, and M. Ido, Physica C **341–348**, 847 (2000).
[16] W. Wang, M. Yamazaki, K. Lee, and I. Iguchi, Phys. Rev. B **60**, 4272 (1999).
[17] I. Iguchi, W. Wang, M. Yamazaki, Y. Tanaka, and S. Kashiwaya, Phys. Rev. B **62**, R6131 (2000).
[18] J. Gao, Y. M. Boguslavskij, B. B. G. Klopman, D. Terpstra, R. Wijbrans, G. J. Gerritsma, and H. Rogalla, J. Appl. Phys. **72**, 1 (1992).
[19] C. Horstmann, P. Leinenbach, A. Engelhardt, R. Dittmann, U. Memmert, U. Harttmann, and A. I. Braginski, IEEE Trans. Appl. Supercond. **2**, 2844 (1997).
[20] T. Satoh, M. Hidaka, and S. Tahara, IEEE Trans. Appl. Supercond. **9**, 3141 (1999).
[21] Y. Tanaka and S. Kashiwaya, Phys. Rev. B **53**, 9371 (1996).
[22] R. C. Dynes, V. Narayanamurti, and J. P. Garno, Phys. Rev. Lett. **41**, 1509 (1978).
[23] A. Ino, C. Kim, M. Nakamura, T. Yoshida, T. Mizokawa, A. Fujimori, Z.-X. Shen, T. Kakeshita, H. Eisaki, and S. Uchida, Phys. Rev. B **65**, 094504 (2002).
[24] H. Sato, A. Tsukada, M. Naito, and A. Matsuda, Phys. Rev. B **61**, 12447 (2000).
[25] Y. Tanaka and S. Kashiwaya, Phys. Rev. Lett. **74**, 3451 (1995).
[26] T. Lofwander, V. S. Shumeiko, and G. Wendin, Supercond. Sci. Technol. **14**, R53 (2001).
[27] Yu. S. Barash, A. A. Svidzinsky, and H. Burkhardt, Phys. Rev. B **55**, 15282 (1997).
[28] Y. Tanaka (unpublished).
[29] A. Matsuda, S. Sugita, and T. Watanabe, Phys. Rev. B **60**, 1377 (1999).
[30] T. Sato, T. Yokaya, Y. Naitoh, T. Takahashi, K. Yamada, and Y. Endo, Phys. Rev. Lett. **83**, 2254 (1999).
[31] N. Miyakawa, P. Guptasarma, J. F. Zasadzinski, D. G. Hinks, and K. E. Gray, Phys. Rev. Lett. **80**, 157 (1998).
[32] V. M. Kransov, A. Yurgens, D. Winkler, P. Delsing, and T. Claeson, Phys. Rev. Lett. **84**, 5860 (2000).
[33] K. M. Lang, V. Madhavan, J. E. Hoffman, E. W. Hudson, H. Eisaki, S. Uchida, and J. C. Davis, Nature (London) **415**, 412 (2001).
[34] T. Cren, D. Roditchev, W. Sacks, J. Klein, J.-B. Moussy, C. Deville-Cavellin, and M. Lagues, Phys. Rev. Lett. **84**, 147 (2000).